

An MNG-TL Loop Antenna for UHF Near-Field RFID Applications

Hu Liu*, Ying Liu, Ming Wei, and Shuxi Gong

Abstract—A loop antenna is designed and fabricated for ultra-high frequency (UHF) near-field radio frequency identification (RFID) readers. The artificial mu-negative transmission line (MNG-TL) structure has been applied to the antenna design, which will help the current distribution along the loop to keep in phase even with the perimeter of the loop more than two operating wavelengths. Thus a strong and uniform magnetic field distribution in the near field of the antenna can be generated. The simulated and measured results indicate that a relatively large impedance bandwidth from 762 MHz to 1048 MHz has been obtained. The overall size of the antenna is 216 mm \times 216 mm \times 0.4 mm, and a large interrogation zone with uniform and strong magnetic field distribution of up to 187.2 mm \times 187.2 mm has been achieved.

1. INTRODUCTION

Radio frequency identification (RFID) has been widely used in tracking technology and wireless identification. Recently, due to the promising applications in item-level RFID systems, UHF near-field technology has received much attention [1–4]. Nevertheless, with the perimeter of the loop antenna comparable to the operating wavelength, inverse current or phase-inversion will make the antenna unable to generate uniform and strong magnetic field distribution [5]. To deal with this kind of problems, a segmented loop antenna loaded with lumped capacitor was presented in [6]. The structure of segmented loops with dashed lines is applied in the antenna design in [7–9] by Qing et al.. A relatively large interrogation zone has been obtained with this structure. Distributed capacitors are used in [10] to realize in-phase current.

Recently left-handed materials (LHMs) and artificial magnetic conductor (AMC) have received a lot of attention due to their roles in antenna size reduction and improvement of radiation patterns [11–13]. The MNG-TL is an artificial structure which can restrain the current reversal. Taking this property into consideration, MNG-TL has been applied to realize horizontally polarized omnidirectional loop antenna array in [14]. Meanwhile, MNG-TL was utilized to improve the current distribution and help obtain stable radiation patterns for a wideband dipole antenna in [15].

In this paper, the MNG-TL structure has been used to design a UHF near-field RFID loop antenna to restrain the phase-inversion and current nulls. A broad bandwidth and a large interrogation zone with even and strong magnetic field distribution have been obtained.

2. DESIGN AND ANALYSIS

2.1. Antenna Configuration

Figure 1 shows the configuration of the proposed MNG-TL loop antenna. The overall size of the antenna is 216 mm \times 216 mm \times 0.4 mm and an interrogation zone of up to 187.2 mm \times 187.2 mm has been offered.

Received 5 February 2015, Accepted 19 March 2015, Scheduled 24 March 2015

* Corresponding author: Hu Liu (liuhu@stu.xidian.edu.cn).

The authors are with the National Laboratory of Science and Technology on Antennas and Microwaves, Xidian University, Xi'an, Shanxi 710071, China.

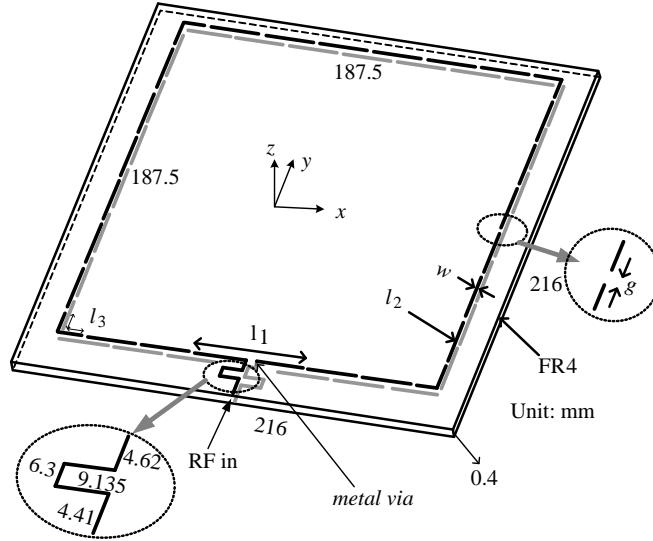


Figure 1. Overall configuration of the proposed MNG-TL loop antenna.

Table 1. Detailed dimensions of the proposed antenna.

Parameters	l_1	l_2	l_3	w	g
Value (mm)	54.48	25.20	23.52	1.68	1.2

The antenna consists of a certain quantity of periodically loaded parallel-plate lines. The parallel-plate line is composed of two parallel conducting strips, which are respectively printed onto the lower and upper side of an FR4 substrate ($\epsilon_r = 4.4$). The conducting strips on both sides of the substrate have a length of l_2 . g is the gap between the conducting strips on the same side. A parallel strip line printed on the upper and lower side of the substrate respectively is connected to the 50- Ω coaxial cable to feed the antenna. The thickness of the substrate is 0.4 mm. The lower strip line is connected with the upper part of the conducting strip through a metal via. To achieve better impedance match, the feeding parallel strip line is set to be meandered. The specific dimensions of the antenna are illustrated in Table 1.

2.2. MNG-TL Structure

When the perimeter of the loop antenna is more than two operating wavelengths, due to the occurrence of the reverse current, the magnetic field generated by the adjacent sides of the conventional solid-line loop antenna will be canceled out by each other. Consequently, the magnetic field over the loop antenna cannot be kept even and the central part of the interrogation zone will suffer very weak magnetic field distribution.

The composite right/left-handed transmission line has been analyzed comprehensively in some previous literatures. An equivalent circuit mode has been illustrated in Figure 2 to further understand the working principle of the proposed antenna. The circuit consists of a series inductance L_R and a shunt capacitance C_R to represent the distributed inductance and capacitance of the transmission line (TL) section. The parallel-plate TL sections have the same characteristic impedance Z_a . Meanwhile a series capacitance C_L has also been added to the model to represent the coupling effects between the adjacent conducting strips on the same side of the substrate. It can be observed that the left-handed series capacitance C_L has been periodically added to the antenna structure, which gives the indication that the proposed antenna owns a mu-negative transmission line (MNG-TL) structure. The theoretical analysis has been conducted in detail in [16].

The previous literatures [17, 18] have proven that an infinite wavelength at the zeroth-order resonance ($\beta = 0, \omega \neq 0$) can be obtained by the MNG-TL structure, where the effective permeability is

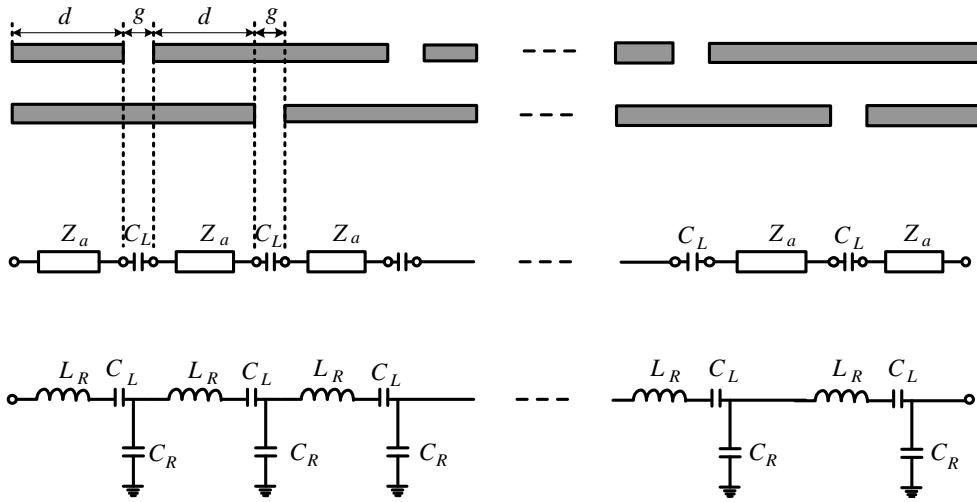


Figure 2. The equivalent circuit of the MNG-TL structure.

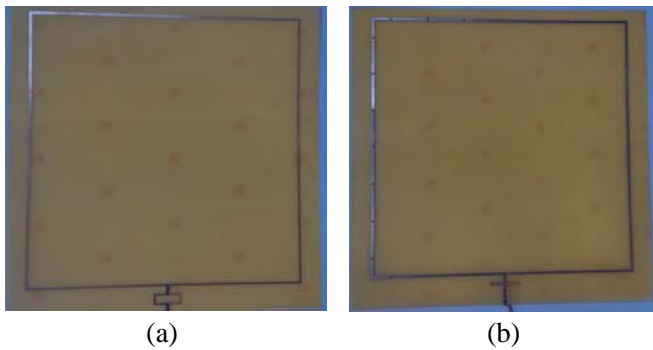


Figure 3. Photograph of (a) the conventional loop antenna, (b) the proposed MNG-TL loop antenna.

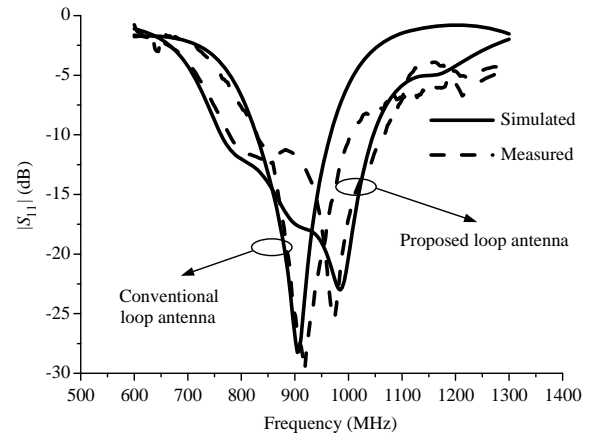


Figure 4. Simulated $|S_{11}|$ against frequency of the proposed antenna.

zero. And there is no phase shift across the resonator for the phase shift is determined by $\varphi = \beta d$, where d is the periodical length of TL sections. Therefore, by utilizing the MNG-TL structure, the proposed loop antenna can realize a zero propagation constant with non-zero group velocity at the zeroth-order resonance, which will restrain the current reversal and thus improve the current distribution. Meanwhile, the MNG-TL can be useful to help the antenna to obtain large bandwidth [15].

3. RESULT AND DISCUSSION

To verify the properties of the proposed antenna, a prototype has been fabricated and tested. The photograph of the antenna is given in Figure 3(a). As is shown in Figure 3(b), a conventional solid-line loop antenna with the same size of the proposed antenna is also fabricated for comparison.

3.1. Impedance Bandwidth

Figure 4 gives the simulated and measured $|S_{11}|$ of the proposed and conventional loop antenna against frequency. It can be observed from the measured results that a relative impedance bandwidth of up to 31.6% from 762 MHz to 1048 MHz, within which $|S_{11}|$ is below -10 dB, has been achieved. A

relatively large impedance bandwidth compared to the conventional loop antenna has been achieved by the proposed antenna. The little discrepancy between the simulated and measured results can be caused by fabrication error and measurement tolerance.

3.2. Current and Magnetic Field Distributions

The simulated current distribution of the conventional solid-line loop antenna and the proposed antenna at 915 MHz are demonstrated in Figure 5. It can be observed from Figure 5(a) that reverse current occurs along the conventional loop antenna. While Figure 5(b) shows that the MNG-TL structure has led to an in-phase current distribution along the loop antenna, and meanwhile the current magnitude is almost equal. As a result, the magnetic field distribution in the near zone of the antenna will be uniform and strong.

Figure 6 gives the simulated 2-D magnetic field distribution of the conventional solid-line loop antenna and the proposed MNG-TL loop antenna at 915 MHz. It can be indicated from Figure 6(a) that the current reversal along the antenna loop has resulted in an uneven magnetic field distribution and a sharp reduction of the magnetic field in the central portion of the interrogation zone can be observed for the fact that the magnetic field generated by the currents on the adjacent conducting strips will be weakened by each other due to the existence of the inverse current. Meanwhile, it can be observed from Figure 6(b) that strong and even magnetic field distribution over the interrogation zone has been obtained, owing to the fact that MNG-TL structure has achieved the in-phase current along the loop, which will ensure the realization of the uniform field distributions even with the antenna perimeter more than two operating wavelengths.

The simulated magnetic field distributions of the conventional loop antenna and the proposed

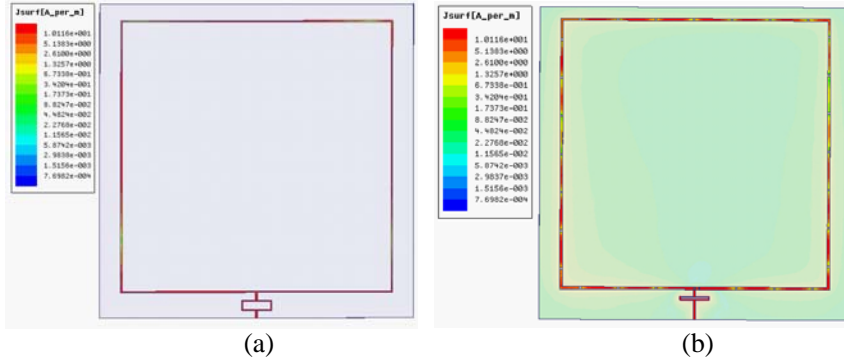


Figure 5. Simulated current distribution along (a) the conventional loop antenna, (b) the proposed MNG-TL loop antenna at 915 MHz.

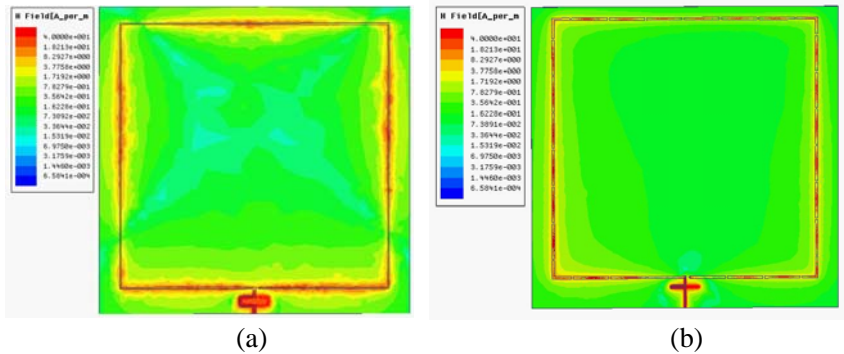


Figure 6. Simulated 2-D magnetic field distribution of (a) the conventional loop antenna and (b) proposed loop antenna at 915 MHz.

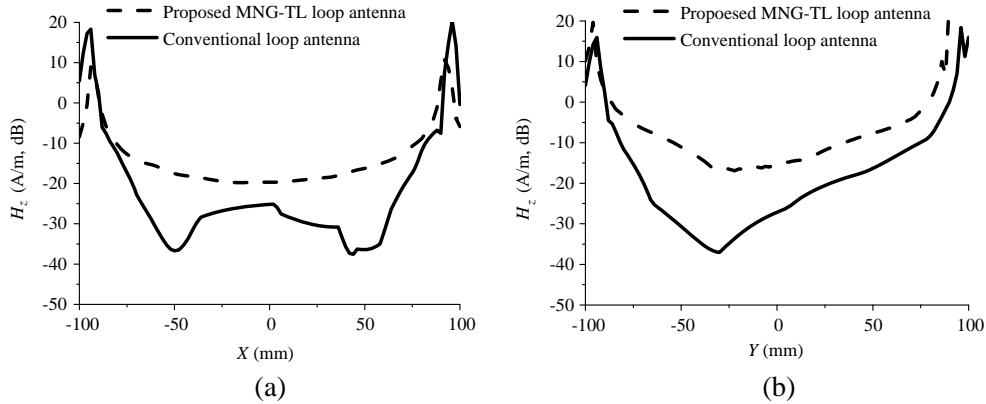


Figure 7. Simulated magnetic field distribution of the conventional loop antenna and proposed MNG-TL loop antenna at 915 MHz. ($z = 0.1$ mm): (a) x -axis variation, (b) y -axis variation.

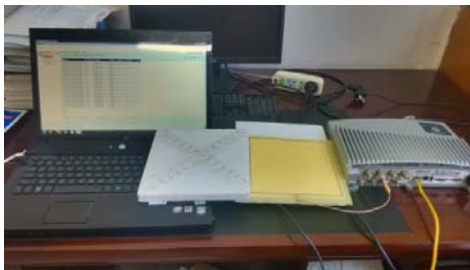


Figure 8. Measurement set-up of Motorola R440 reader and the proposed MNG-TL loop antenna.

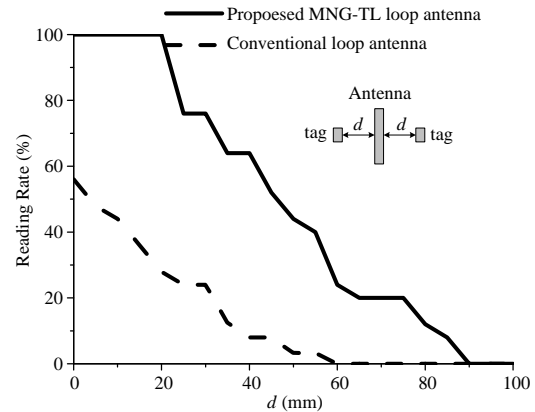


Figure 9. Measured reading rate against distance of the conventional loop antenna and proposed MNG-TL loop antenna.

MNG-TL loop antenna are given in Figure 7. The magnetic field distributions along the x -axis and y -axis are illustrated in Figure 7(a) and Figure 7(b) respectively. It can be clearly shown that a sharp reduction of the magnetic field has occurred in the central part of the conventional loop antenna, which is in accordance with the magnetic distribution indicated from Figure 6(a). Instead Figure 7(b) indicates that for the proposed MNG-TL antenna, the magnetic field distribution remains strong and uniform over the main part of the interrogation zone.

Figure 7 shows that a variation of less than 5 dB and more than 20 dB has been observed over the major portion of the interrogation by the proposed and conventional loop antenna, respectively. The slight asymmetry of the magnetic distribution in Figure 7(b) can be caused by the asymmetrical structure of the antenna along the y -axis. The maximum variations of the magnetic field over the main part of the interrogation zone (-75 mm $< x, y < 75$ mm) for the proposed and conventional loop antenna are 10 dB and 38 dB, respectively. It can be concluded that a large interrogation zone with a strong and uniform magnetic field distribution has been achieved by the proposed antenna.

3.3. Simulated and Measured Reading Rate

To investigate the reading range of the proposed antenna, the MNG-TL antenna is connected to the Motorola R440 reader and used as the reader antenna to detect the RFID tags. The whole measurement set-up is shown in Figure 8. 25 tags are placed symmetrically on a cubic polystyrene foam board. When

the foam is held right above and some distance away from the antenna, the number of tags that can be detected will be displayed and recorded.

The measured reading rate against reading range of the proposed MNG-TL loop antenna and the conventional loop antenna is illustrated in Figure 9. It clearly shows that the proposed antenna can achieve a 100% reading rate at a distance of up to 20 mm, which also can indicate that a strong and even magnetic field distribution in the near zone of the proposed antenna has been obtained. While for the conventional loop antenna, due to the weak magnetic field distribution in the central part of the antenna, a 100% reading rate has not been observed even when the tags are placed right on the antenna ($d = 0$ mm).

4. CONCLUSION

The MNG-TL has been applied to design a loop antenna to restrain the current reversal and thus to improve the magnetic field distribution in the vicinity of the antenna. A relatively broad impedance bandwidth from 762 MHz to 1048 MHz has been achieved for UHF RFID applications. Due to the MNG-TL structure, a strong and uniform magnetic field distribution has been observed and a large interrogation zone of up to $187.2\text{ mm} \times 187.2\text{ mm}$ has been obtained with the perimeter of the loop antenna more than two operating wavelength. Meanwhile, a relatively long reading range of up to 20 mm with a 100% reading rate has also been obtained. The proposed antenna can be a good candidate for the reader antennas in the UHF near-field RFID systems.

ACKNOWLEDGMENT

This work is supported by the Program for New Century Excellent Talents in University (NCET-11-0690), the Fundamental Research funds for the Central Universities (K5051202049), and the National Natural Science Foundation of China (No. 61372001).

REFERENCES

1. Finkenzeller, K., *RFID Handbook*, 2nd edition, Wiley, New York, NY, USA, 2004.
2. Landt, J., "The history of RFID," *IEEE Potentials*, Vol. 24, No. 4, 8–11, Oct.–Nov. 2005.
3. Fan, Z., S. Qiao, J. T. Huang-Fu, and L.-X. Ran, "A miniaturized printed dipole antenna with V-shaped ground for 2.45 GHz RFID readers," *Progress In Electromagnetics Research*, Vol. 71, 149–158, 2007.
4. Tsai, M.-C., C.-W. Chiu, H.-C. Wang, and T.-F. Wu, "Inductively coupled loop antenna design for UHF RFID on-body applications," *Progress In Electromagnetics Research*, Vol. 143, 315–330, 2013.
5. Nikitin, P. V., K. V. S. Rao, and S. Lazar, "An overview of near field UHF RFID," *Proc. IEEE Int. Conf. on RFID*, 167–174, Mar. 2007.
6. Dobkin, D. M., S. M. Weigand, and N. Iyec, "Segmented magnetic antennas for near-field UHF RFID," *Microw. J.*, Vol. 50, No. 6, Jun. 2007.
7. Qing, X., C. K. Goh, and Z. N. Chen, "Segmented loop antenna for UHF near-field RFID applications," *Electron. Lett.*, Vol. 45, No. 17, Aug. 2009.
8. Qing, X., C. K. Goh, and Z. N. Chen, "A broadband UHF near-field RFID antenna," *IEEE Trans. Antennas Propag.*, Vol. 58, No. 12, 3829–3838, Dec. 2010.
9. Ong, Y. S., X. Qing, C. K. Goh, and Z. N. Chen, "A segmented loop antenna for UHF near-field RFID," *Proc. IEEE Antennas Propag. Soc. Int. Symp.*, 1–4, 2010.
10. Qing, X., Z. N. Chen, and C. K. Goh, "UHF near-field RFID reader antenna with capacitive couplers," *Electron. Lett.*, Vol. 46, No. 24, 1591–1592, Dec. 2010.
11. Ziolkowski, R. W. and A. Erentok, "Metamaterial-based efficient electrically small antennas," *IEEE Trans. Antennas Propag.*, Vol. 54, No. 7, 2113–2130, Jul. 2006.

12. Goussetis, G., A. P. Feresidis, and J. C. Vardaxoglou, "Periodically loaded dipole array supporting left-handed propagation," *Proc. IEEE Microw., Antennas, Propag.*, Vol. 152, 251–254, Aug. 2005.
13. Ziolkowski, R. W., "Design, fabrication, and testing of double negative metamaterials," *IEEE Trans. Antennas Propag.*, Vol. 51, No. 7, 1516–1529, Jul. 2003.
14. Wei, K., Z. Zhang, F. Zheng, and M. F. Iskander, "A MNG-TL loop antenna array with horizontally polarized omnidirectional patterns," *IEEE Trans. Antennas Propag.*, Vol. 60, No. 6, 2702–2710, Jun. 2012.
15. Wei, K., Z. Zhang, Z. Feng, and M. F. Iskander, "A wideband MNG-TL dipole antenna with stable radiation patterns," *IEEE Trans. Antennas Propag.*, Vol. 61, No. 5, 2418–2424, May 2013.
16. Wei, K., Z. Zhang, Z. Feng, and M. F. Iskander, "A MNG-TL loop antenna array with horizontally polarized omnidirectional patterns," *IEEE Trans. Antennas Propag.*, Vol. 60, No. 6, 2702–2710, Jun. 2012.
17. Caloz, C. and T. Itoh, *Electromagnetic Metamaterials: Transmission Line Theory and Microwave Applications*, Wiley-IEEE Press, Hoboken-Piscataway, NJ, USA, 2005.
18. Park, J.-H., Y.-H. Ryu, and J.-J. Li, "Mu-zero resonance antenna," *IEEE Trans. Antennas Propag.*, Vol. 58, No. 6, 1865–1875, Jun. 2010.